NOTES AND CORRESPONDENCE

On the Relationship between Tropical and North Pacific Sea Surface Temperature Variations

CLARA DESER

CIRES, University of Colorado, Boulder, Colorado

MAURICE L. BLACKMON

Climate Diagnostics Center, NOAA, Boulder, Colorado

9 February 1994 and 4 October 1994

ABSTRACT

Empirical orthogonal function analysis of winter sea surface temperature (SST) anomalies over the Pacific domain (60°N–20°S) reveals an El Niño–Southern Oscillation (ENSO) mode that is linked to the eastern North Pacific, and a North Pacific mode that is linearly independent of ENSO. The North Pacific mode exhibits maximum amplitude and variance explained along ~40°N, west of ~170°W. SSTs in this region have decreased by ~1.5°C from 1950 to 1987. The cooling in winter has been associated with a strengthening of the overlying westerly winds.

1. Introduction

The tendency for tropical Pacific sea surface temperature (SST) anomalies during El Niño/Southern Oscillation (ENSO) events to be associated with SST anomalies in the North Pacific has been emphasized in many studies (Weare et al. 1976; Hsiung and Newell 1983; Pan and Oort 1983, 1990; Alexander 1990, 1992; Lau and Nath 1994). The SST linkage is thought to occur via an atmospheric "bridge," whereby anomalous convection over the equatorial Pacific associated with anomalous SSTs induces a remote atmospheric circulation response over the North Pacific; these circulation anomalies in turn force local SST anomalies via mixed layer dynamics (Alexander 1990, 1992; Luksch and von Storch 1992; Lau and Nath 1994). This "atmospheric bridge" is expected to operate most effectively during winter when the mean flow in the Tropics and subtropics is favorable for Rossby wave propagation. The purpose of this study is to reexamine the relationship between tropical and North Pacific SST anomalies during winter. How strong is the connection between North Pacific SST variations and ENSO? To what extent do SSTs in the North Pacific vary independently from those in the tropical Pacific? What are the atmospheric teleconnection patterns associated with tropical and North Pacific SST variations?

Corresponding author address: Dr. Clara Deser, CIRES, University of Colorado, Campus Box 449, Boulder, CO 80309.

2. Data and methods

The SST and surface wind data used in this study are from the recently updated Comprehensive Ocean–Atmosphere Data Set (COADS); see Woodruff et al. (1987) for a description. Monthly data on a 4° × 4° latitude/longitude grid for the period January 1950–December 1992 are used. Note that the database for the 1980–1992 period has been significantly enhanced relative to the previous COADS release (Woodruff et al. 1993). Monthly anomalies were defined by subtracting the long-term means from each month. The monthly anomalies were then averaged to form winter (November–March) anomalies. Empirical orthogonal function analysis was used to identify objectively the dominant modes of variability of winter SST anomalies over the Pacific from 60°N to 20°S. Monthly mean 500-mb geopotential height data from the National Center for Atmospheric Research data library are also used. These data span the period 1950–1992.

3. Results

a. EOF analysis of Pacific SSTs

Figure 1 shows the first two empirical orthogonal functions (EOFs) of winter SST anomalies over the Pacific Ocean from 60°N to 20°S. The EOFs are based on the covariance matrix and are shown in normalized form (i.e., correlation coefficients between the time series of each EOF and the original data). The first mode

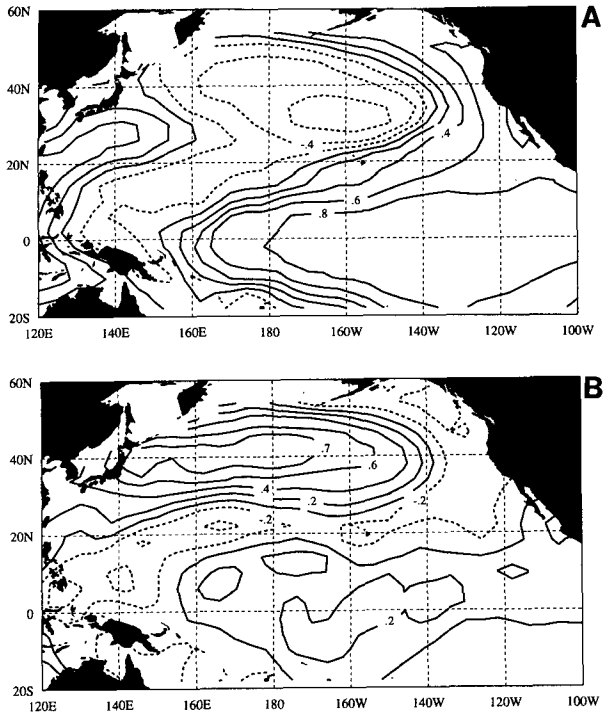

FIG. 1. (a) EOF 1 of Pacific SSTs based on winter (November–March) anomalies during the period 1950/51–1991/92. The EOF is based on the covariance matrix and is shown in normalized form (i.e., correlation coefficients between the time series of the EOF and the original data). The contour interval is 0.2 and negative contours are dashed. (b) As in (a) but for EOF 2. The 0.7 contour is also shown.

(Fig. 1a) explains 43% of the variance over the domain. The strongest correlations ($r > 0.9$) are found in the eastern tropical Pacific. The largest negative correlations are ~ -0.65 in the vicinity of 30°N, 165°W. This pattern is very similar to the first nonseasonal EOF of Weare et al. (1976) and Hsiung and Newell (1983) based on a shorter period of record. The second EOF (Fig. 1b) is primarily a North Pacific mode, with the strongest correlations ($r > 0.7$) located along 40°N, west of 170°W. It exhibits negligible correlation with the tropical Pacific. EOF 2 explains 11% of the variance over the domain. Rotation of the EOFs according to the varimax criterion (see Horel 1981) does not significantly alter the patterns shown in Fig. 1. The leading EOFs for winter defined as January–March or December–February are similar to those for November–March.

The time series of winter (November–March) SST anomalies averaged over the centers of action of rotated EOFs 1 and 2 are shown in Figs. 2a and 2b, respectively. The region 6°N–6°S, 178°–106°W is used to represent EOF 1, and 46°–32°N, 136°E–176°W represents EOF 2. These regional SST indices are virtually indistinguishable from the time series of the rotated EOFs themselves (e.g., the correlation between EOF 1 and the equatorial Pacific SST index is 0.97; similarly the correlation between EOF 2 and the North Pacific SST index is also 0.97). The equatorial Pacific SST index (Fig. 2a) exhibits extremes during ENSO years as well as a long-term "shift" toward higher values starting in 1976/77. The relative warmth of the tropical Pacific since 1976 has been noted by Trenberth and Hurrell (1994), Graham (1993), and Lau and Nath (1994), among others. The North Pacific SST index (Fig. 2b) exhibits a long-term cooling trend from the mid-1950s to the mid-1980s, followed by an apparent recovery in the most recent three years. Alternatively, the North Pacific SST index exhibits a discrete warm period (1950–57) and a cool period (1973–89). The correlation between the two time series is −0.20, not significantly different from zero. The timescale for the North Pacific index is noticeably longer than that for the equatorial Pacific index.

b. Relation of SST EOFs to 500-mb geopotential heights

Figures 3a and 3b show the winter 500-mb height anomaly patterns associated with a one standard de-

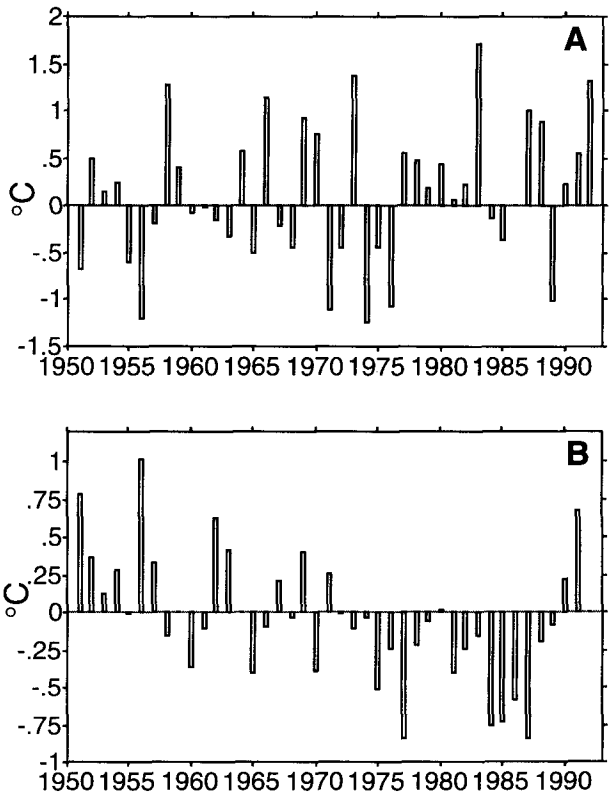

FIG. 2. Time series of winter SST anomalies averaged over the centers of action of the EOFs. (a) Equatorial Pacific SST index, 6°N–6°S, 178°–106°W. (b) North Pacific SST index, 46°–32°N, 136°E–176°W. Winter is defined as November–March; the year corresponds to that of January. The correlation coefficient between the SST index and the corresponding (rotated) EOF time series is 0.97 for both EOFs.

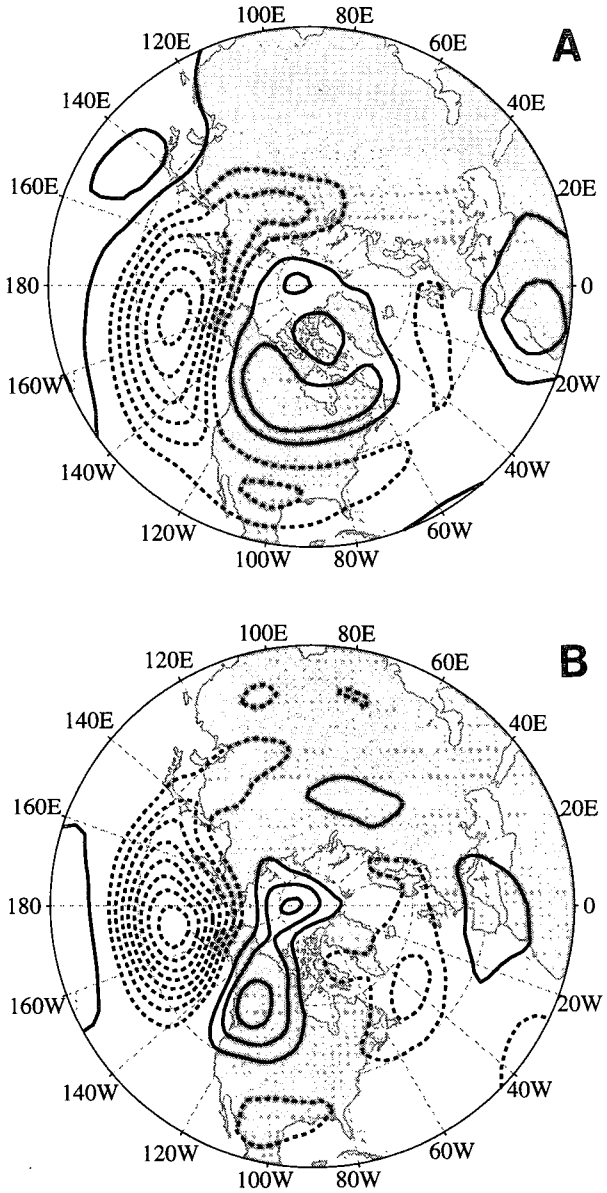

FIG. 3. Winter (November–March) 500-mb geopotential height anomaly patterns associated with a one standard deviation departure of the (a) equatorial Pacific SST index and (b) North Pacific SST index. The patterns were obtained by regressing the winter 500-mb height anomalies upon the SST index and multiplying the regression coefficients by the index standard deviation (0.75°C for the equatorial Pacific SST index and 0.43°C for the North Pacific SST index). Contour interval: 5 m; negative contours are dashed and the zero contour is omitted. Note that the sign of the 500-mb pattern in (b) is reversed for clearer comparison with (a).

viation departure of the equatorial Pacific SST index and the North Pacific SST index, respectively. The patterns were obtained by regressing the winter 500-mb height anomalies upon the SST index and multiplying the regression coefficients by the index standard deviation (0.75°C for the equatorial Pacific SST index and 0.43°C for the North Pacific SST index). Note that the sign of 500-mb anomaly pattern based on the North Pacific SST index is reversed so that it may be readily compared with the pattern based on the equatorial Pacific SST index. The gross features of the two 500-mb patterns are similar: the largest height anomalies occur in the vicinity of the Aleutian low, with weaker anomalies of the opposite polarity over northwestern Canada and the subtropical Pacific. The maximum height anomalies immediately south of the Aleutian Islands are ~30 m for the equatorial Pacific SST index and ~40 m for the North Pacific SST index. Differences between the two patterns are also evident: the negative height anomalies associated with the equatorial Pacific index (Fig. 3a) exhibit a northwest–southeast tilt over the North Pacific and the subtropical anomalies are located in the far western Pacific, whereas the height anomalies associated with the North Pacific index exhibit a structure that more closely resembles the Pacific/North American (PNA) pattern (Wallace and Gutzler 1981). The 500-mb height patterns shown in Figs. 3a and 3b are consistent with the results of Wallace and Jiang (1987), which were based on a subjective selection of SST indices.

c. *Relation of SST EOFs to surface winds*

To ascertain to what extent surface fluxes may be important in forcing the SST anomalies over the North Pacific that are associated with EOFs 1 and 2, surface wind anomaly patterns associated with a one standard deviation departure of the equatorial Pacific index and the North Pacific index are shown in Figs. 4a and 4b,

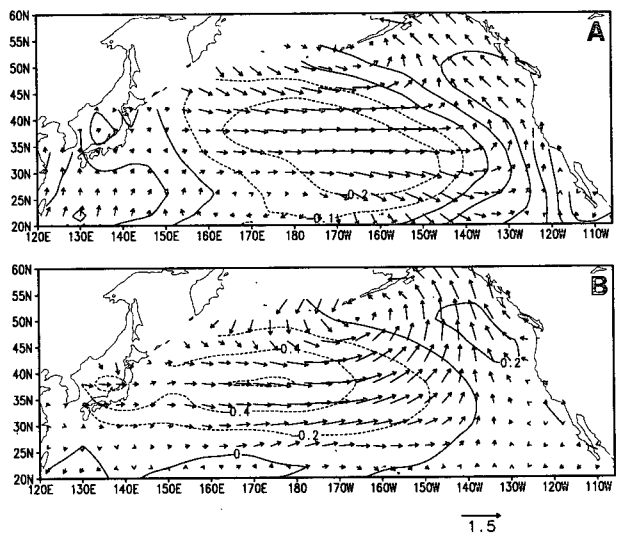

FIG. 4. Winter surface wind (vectors) and SST (contours) anomaly patterns associated with a one standard deviation departure of the (a) equatorial Pacific SST index and (b) North Pacific SST index. Contour interval: 0.1°C in (a) and 0.2°C in (b). Wind scale (m s^{-1}) given in lower right. Note that the signs of the wind and SST patterns in (b) are reversed for clearer comparison with (a).

respectively. The wind patterns were derived following the method used for 500-mb height. As Cayan (1992) and Lau and Nath (1994) have shown, surface winds give a reasonable guide to the net surface fluxes in midlatitudes during winter. Figure 4 shows that the North Pacific component of both SST modes underlie zonal wind anomalies, such that when the westerlies are stronger, SSTs are cooler and vice versa. Stronger winds can cool the ocean mixed layer by enhancing the fluxes of sensible and latent heat, intensifying entrainment and enhancing cold advection by Ekman currents in regions where the mean poleward SST gradient is strong, such as along 40°N. Note that the more zonal orientation of the SST anomalies associated with EOF 2 compared with EOF 1 is consistent with the surface wind anomaly patterns. Thus, it appears that for both EOFs, the North Pacific SST component may be forced at least in part by changes in the atmospheric circulation.

4. Summary

The leading EOF of winter SST anomalies over the Pacific Ocean from 60°N to 20°S is the ENSO mode with a connection to the eastern North Pacific, in keeping with results of previous studies. The strongest extratropical correlations for this mode are ~−0.65 in the vicinity of 30°N, 165°W and ~0.8 along Baja, California. The second EOF is a North Pacific mode that is linearly independent of ENSO. This mode exhibits maximum amplitude and variance explained along ~40°N, west of ~170°W. SSTs in this region have decreased by ~1.5°C from 1950 to 1987. The cooling has been associated with a strengthening of the overlying westerly winds. The North Pacific SST mode is associated with the PNA teleconnection pattern in the midtroposphere.

Similar SST modes have been reported independently by Kawamura (1994), who computed rotated EOFs of the global SST field based on monthly data. His results suggest the long-term cooling of the North Pacific occurred in conjunction with a warming of the tropical Indian Ocean. Further study is needed to determine the nature of this association.

Acknowledgments. We thank the reviewers for their helpful suggestions. This study was supported by a grant from the NOAA Office of Global Programs.

REFERENCES

Alexander, M. A., 1990: Simulation of the response of the North Pacific Ocean to the anomalous atmospheric circulation associated with El Niño. *Climate Dyn.*, **5,** 53–65.

——, 1992: Midlatitude atmosphere–ocean interaction during El Niño. Part I: The North Pacific Ocean. *J. Climate,* **5,** 944–958.

Cayan, D. R., 1992: Latent and sensible heat flux anomalies over the northern oceans: Driving the sea surface temperature. *J. Phys. Oceanogr.*, **22,** 859–881.

Graham, N. E., 1993: Decadal-scale climate variability in the 1970s and 1980s: Observations and model results. *Climate Dyn.*, submitted.

Horel, J. D., 1981: A rotated principal component analysis of the interannual variability of the Northern Hemisphere 500 mb height field. *Mon. Wea. Rev.*, **109,** 2080–2092.

Hsuing, J., and R. E. Newell, 1983: The principal nonseasonal modes of variation of global sea surface temperature. *J. Phys. Oceanogr.*, **13,** 1957–1967.

Kawamura, R., 1994: A rotated EOF analysis of global sea surface temperature variability with interannual and interdecadal scales. *J. Phys. Oceanogr.*, **24,** 707–715.

Lau, N.-C., and M. J. Nath, 1994: A modeling study of the relative roles of tropical and extratropical SST anomalies in the variability of the global atmosphere–ocean system. *J. Climate,* **7,** 1184–1207.

Luksch, U., and H. von Storch, 1992: Modeling the low-frequency sea surface temperature variability in the North Pacific. *J. Climate,* **5,** 893–906.

Pan, Y. H., and A. H. Oort, 1983: Global climate variations connected with sea surface temperature anomalies in the eastern equatorial Pacific Ocean for the 1958–73 period. *Mon. Wea. Rev.*, **111,** 1244–1258.

——, and ——, 1990: Correlation analyses between sea surface temperature anomalies in the eastern equatorial Pacific and the World Ocean. *Climate Dyn.*, **4,** 191–205.

Trenberth, K. E., and J. W. Hurrell, 1994: Decadal atmosphere–ocean variations in the Pacific. *Climate Dyn.*, **9,** 303–319.

Wallace, J. M., and D. S. Gutzler, 1981: Teleconnections in the geopotential height field during the Northern Hemisphere winter. *Mon. Wea. Rev.*, **109,** 784–812.

——, and Q.-R. Jiang, 1987: On the observed structure of the interannual variability of the atmosphere/ocean climate system. *Atmospheric and Oceanic Variability.* H. Cattle, Ed., Roy. Meteor. Soc., 17–43.

Weare, B. C., A. Navato, and R. E. Newell, 1976: Empirical orthogonal function analysis of Pacific Ocean sea surface temperatures. *J. Phys. Oceanogr.*, **6,** 671–678.

Woodruff, S. D., R. J. Slutz, R. L. Jenne, and P. M. Steurer, 1987: A Comprehensive Ocean–Atmosphere Data Set. *Bull. Amer. Meteor. Soc.*, **68,** 521–527.

——, S. J. Lubker, K. Wolter, S. J. Worley, and J. D. Elms, 1993: Comprehensive Ocean–Atmosphere Data Set (COADS) release 1a: 1980–92. *Earth System Monitor,* **4,** 1–8.